Electronic Supplementary Material (ESI) for Chemical Communications.
This journal is © The Royal Society of Chemistry 2015

Electronic Supplementary Information (ESI)

Unique electrocatalytic activity of nucleic acid-mimicking coordination polymer for sensitive detection of coenzyme A and histone acetyltransferase activity

Yufang Hu, Siyu Chen, Yitao Han, Hongjun Chen, Qin Wang, Zhou Nie,* Yan Huang, Shouzhuo Yao

State Key Laboratory of Chemo/Biosensing and Chemometrics, College of Chemistry and Chemical Engineering, Hunan University, Changsha, 410082, P. R. China. Fax: +86-731-88821848; Tel: +86-731-88821626; E-mail: niezhou.hnu@gmail.com

EXPERIMENTAL SECTION

1. Materials

Graphite powder (99.99995%, 325 mesh) was purchased from Alfa Aesar. The preparation of graphene oxide (GO) was custom-synthesized by Hummer's method.[1] HAT (p300, >95%, SDS-PAGE, solution in 50 mM Tris-HCl, pH 7.5, containing 100 mM sodium chloride, 0.2% NP-40, 50 mM imidazole, and 10% glycerol), coenzyme A sodium salt hydrate (CoA), acetyl coenzyme A (Ac-CoA), and anacardic acid were obtained from Sigma-Aldrich (Shanghai, China). The substrate peptide P (RGKGGKGLGKGGAKA) was custom-synthesized by GL Biochem (Shanghai). Poly-A RNA (20 nt) was custom-synthesized by Takara (Dalian, China). All solutions were prepared with ultrapure water (18.3 MΩ cm) from the Millipore Milli-Q system.

2. Apparatus

Electrochemical measurements were carried out by a CHI 660A electrochemical workstation (Chenhua, Shanghai, China) with a conventional three-electrode cell which

involved a glass carbon working electrode (3 mm in diameter), a platinum foil counter electrode, and a saturated calomel reference electrode (SCE). All the potentials used in this work were with respect to SCE. Fluorescence measurements were performed on a QuantaMaster™ 4 fluorescence spectrometer (PTI). UV-vis absorption spectra were obtained on a Beckman DU-800 spectrophotometer. Fourier transform infrared (FT-IR) spectrometric spectra were recorded on a Nicolet AVATAR FT-IR360 spectrometer. The hydrodynamic size of CoA-Ag(I) CP was determined by dynamic light scattering (DLS) using a Zetasizer 3000 HS particle size analyzer (Malvern, UK). Polyacrylamide gel electrophoresis (PAGE) and agarose gel were scanned by a ChemiDoc™ MP System (Bio-Rad). Atomic force microscope (AFM) images of GO and CoA-Ag(I) CP were scanned using a Multimode 8 AFM (Bioscope system, Brucker).

3. Fabrication of GO-modified electrode

The electrochemical biosensor was prepared as following steps: (i) Prior to surface modification, glassy carbon electrode (GCE, 3 mm diameter) was firstly polished with 1.0, 0.3, and 0.05 μm alumina slurry respectively and washed ultrasonically for 5 min with ultrapure water, ethanol, and ultrapure water in sequence, and dried in air at room temperature; (ii) GO suspension (1.0 $mg \cdot mL^{-1}$) was obtained by ultrasonicating GO in HAc-NaAc (0.2 M, pH 5.0) buffer for 2 h. GO was electrodeposited onto the surface of GCE electrode to obtain the GO-modified electrodes (GO/GCE) by electrochemical reduction of GO cycling from -1.5 to +0.5 V at 10 $mV \cdot s^{-1}$ under stirring for 10 cycles. Then, the as-prepared GO-modified electrodes were used for subsequent detection experiments.

4. Preparation of CoA-Ag(I) CP

The CoA-Ag(I) CP synthesis was carried out in a 100 μL mixture containing freshly prepared aqueous solutions of $AgNO_3$ (100 μM), CoA (100 μM), and phosphate buffer (10 mM, pH 7.0). For complete reaction of reactants, the mixture was incubated at 30 °C with gentle stirring (500 rpm) on a constant temperature magnetic stirrer for 8 min. Then, 10 μL of the prepared CoA-Ag(I) CP solution was dropped onto the GO/GCE surface, and kept for

10 min. Finally, the prepared electrode was rinsed completely with phosphate buffer (10 mM, pH 7.0). Then, the cyclic voltammetry (CV) was conducted in phosphate buffer (100 mM, pH 7.0) containing 5 mM H_2O_2 and recorded from -1.2 to 0 V with a scan rate of 50 $mV \cdot s^{-1}$.

5. Synthesis of CoA-capped Ag nanoclusters

CoA-capped Ag nanoclusters (CoA-AgNCs) were synthesized by adding freshly prepared $NaBH_4$ (0.1 mM, 1 μL) to CoA-Ag(I) CP (100 μM, 99 μL) under vigorous shaking. The shaking was kept for 1 min to make sure that silver ions were adequately reduced. The mixtures were then kept in the dark for 90 min at room temperature. To prove the formation of CoA-AgNCs, the mixture after reaction was taken out for fluorescence measurement according to previous reports.[2, 3]

6. Preparation of Ag(0)/GO/GCE

First, some GO-electrodeposited electrodes (GO/GCE) were prepared by electrochemical reduction of GO cycling from -1.5 to +0.5 V at 10 $mV \cdot s^{-1}$ under stirring for 10 cycles and the detailed fabrication process was displayed in "Fabrication of GO-modified electrode" of Supporting information. Second, the GO/GCE was electrodeposited in the solution containing 1.0 mM $AgNO_3$ and 1.0 mM KNO_3 cycling from -1.2 to 0 V at 10 $mV \cdot s^{-1}$ under stirring for 10 cycles to obtain the electrodeposited Ag(0) nanoparticles-based GO-electrodeposited glass carbon electrode (named as Ag(0)/GO/GCE).

7. Detection of histone acetyltransferases (p300) activity

The transcriptional activator protein p300 is used as model HAT enzyme in our work. A 15 amino acids-long substrate peptide is derived from N-terminal tail of histone H4. HAT p300 catalyzes the transfer of an acetyl group from Ac-CoA to lysine residue of substrate peptide, producing ε-N-acetyl lysine residue and CoA. In the presence of p300 HAT, CoA was produced and interacted with Ag(I) to form CoA-Ag(I) CP, so that HAT activity can be facilely probed by monitoring CoA generation during the acetylation. For HAT activity analysis, p300 at different final concentrations (0, 0.1, 0.5, 1.0, 5.0, 10, 20, 50, 100, 500, and 1000 nM) was incubated with substrate peptide (P) (200 μM), Ac-CoA (500 μM), and $AgNO_3$

(500 μM) in phosphate buffer (10 mM, pH 7.0) with a total volume of 100 μL at 30 °C for 80 min under stirring. After reaction, the mixture was taken out for electrochemical measurement under the conditions identical to those mentioned above.

8. Inhibition of HAT p300 studies

HAT p300 (100 nM), P (200 μM), and anacradic acid at different final concentrations (0, 0.1, 1.0, 5.0, 10, 20, 40, 60, 80, 100, 250, 500, and 1000 μM) were pre-incubated for 10 min at room temperature, and then the reaction was initiated by the addition of Ac-CoA (500 μM) and $AgNO_3$ (500 μM) in phosphate buffer (10 mM, pH 7.0) with a total volume of 100 μL at 30 °C for 80 min. After incubation of the reaction mixture for 80 min, the following electrochemical measurement was then performed as described above.

9. Fluorescence measurement

The preparation of CoA-Ag(I) CP was identical to the experiments section of manuscript, then SGII (1: 100, 2 μL) was added to the CoA-Ag(I) CP solution (100 μM, 98 μL) and incubated for 20 min in dark environment. Afterwards, the fluorescence measurement was conducted with excitation at 494 nm, and the fluorescence intensity was measured at 530 nm which is the maximum emission peak of CoA-Ag(I) CP/SGII.

To prove the binding interaction of CoA-Ag(I) CP and GO, GO (1 $mg \cdot mL^{-1}$, 10 μL) and CoA-Ag(I) CP (100 μM, 90 μL) were mixed, and stirred over 1 h at room temperature, then incubated for 30 min. After that, the mixture was centrifuged at 10000 rpm for 10 min. Subsequently, the supernatant was separated from the precipitate and then SGII was introduced into the supernatant solution. The resulting mixture was monitored by fluorescence measurement. Meanwhile, the precipitate was further used for FI-IR experiment.

10. Gel electrophoresis

A 4% nondenaturing polyacrylamide gel was used for examining the synthetized CoA-Ag(I) CP (100 μM) and run at room temperature in TAE buffer (40 mM Tris-HCl, pH 8.0, 2 mM acetic acid, 2 mM EDTA, 12.5 mM Mg^{2+}). The electrophoresis started with an initial voltage of 30 V for 10 min and maintained at 100 V for 110 min. The gel was stained by SGII

for 20 min and scanned with ChemiDoc™ MP System (Bio-Rad).

We attempted to use a 2% agarose gel to separate our CoA-Ag(I) CP samples (1 mM). The gel was run at room temperature in TAE buffer (40 mM Tris-HCl, pH 8.0, 2 mM acetic acid, 2 mM EDTA, 12.5 mM Mg^{2+}). The samples were stained by SGII for 20 min, then the electrophoresis started with an initial voltage of 30 V for 10 min and maintained at 100 V for 110 min. The gel was scanned with ChemiDoc™ MP System (Bio-Rad).

11. FT-IR measurement

FT-IR measurements were performed with a KBr pellet containing CoA-Ag(I) CP. KBr (50 mg) and CoA-Ag(I) CP (100 μM, 20 μL) were mixed uniformly, and the mixture was dried by irradiating with infrared lamp, then compressed into a KBr pellet.

Later, to further exploring the interaction of GO and CoA-Ag(I) CP, FT-IR measurements of free GO, free CoA-Ag(I) CP and the precipitate of GO and CoA-Ag(I) CP after centrifugation mentioned in above fluorescence experiment were carried out, and the preparation conditions of FT-IR samples were the same as aforementioned except using different kinds of samples.

12. AFM characterization

GO suspension (2 $\mu g \cdot mL^{-1}$) was obtained by ultrasonicating GO in ultrapure water for 5 h. To prove the binding interaction of GO and CoA-Ag(I) CP, GO (2 $\mu g \cdot mL^{-1}$, 27 μL) and different concentrations of CoA-Ag(I) CP (3 μL), such as 100 μM, 500 μM, 1 mM, and 2 mM, were mixed, and stirred over 1 h at room temperature, then incubated for 30 min. After that, the mixture was centrifuged at 10000 rpm for 10 min, and the precipitate after centrifugation was re-dispersed gently into 30 μL ultrapure water. Afterwards, the mixture (10 μL) was dropped to the surface of freshly cleaved micas and incubated for 20 min. Finally, the prepared micas were washed with ultrapure water and dried in air for AFM characterization.

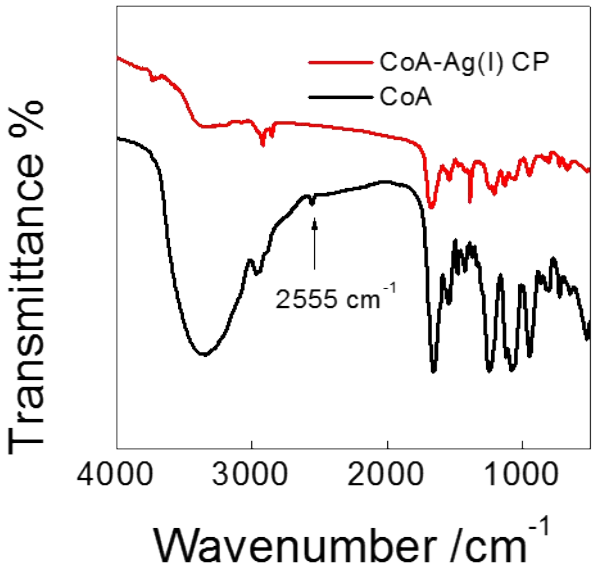

Figure S1 FT-IR spectra of CoA and CoA-Ag(I) CP. [CoA] = [Ag(I)] = 100 μM.

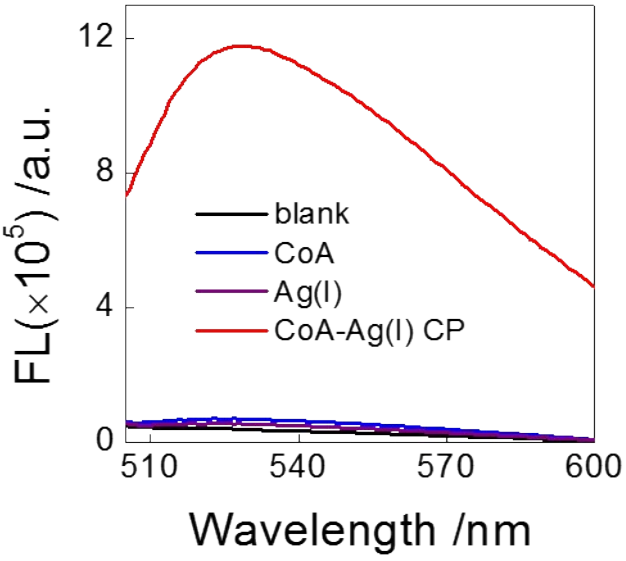

Figure S2 Fluorescence spectra of sole CoA (blue), sole Ag(I) (purple) and the as-prepared CoA-Ag(I) CP (red) (λ_{ex} = 494 nm) in the presence of SGII. The blank (black) is the SGII-only solution. [CoA] = [Ag(I)] = 100 μM.

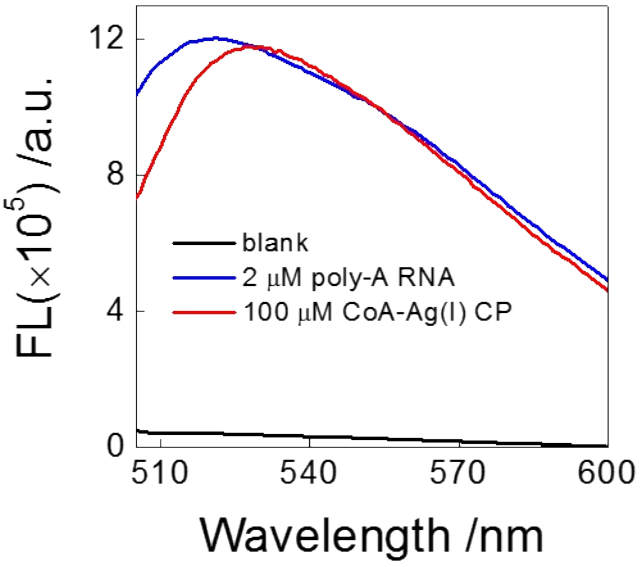

Figure S3 Fluorescence spectra of SGII alone (black), 2 μM 20 nt poly-A RNA stained by SGII (blue), and 100 μM CoA-Ag(I) CP (red) in the presence of SGII. [CoA] = [Ag(I)] = 100 μM.

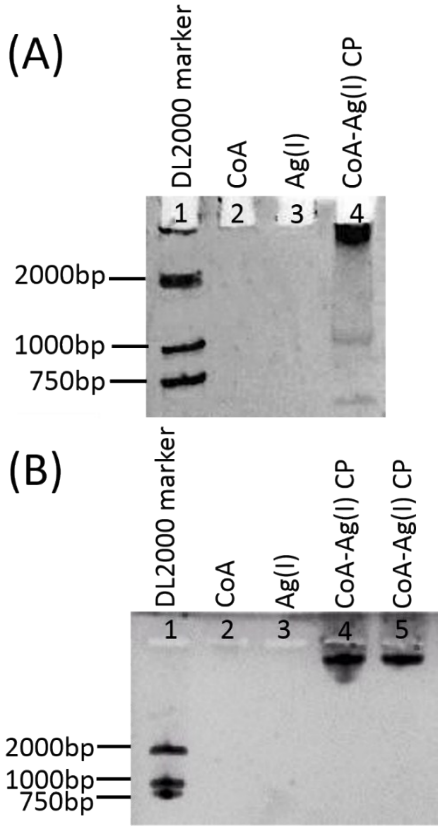

Figure S4 (A) 4% PAGE and (B) 2% agarose gel images for characterizing CoA-Ag(I) CP.

Because the 2% agarose gel (Figure S4B) is able to separate biomolecules with larger molecular weight compared with the 4% PAGE gel (Figure S4A), most of CoA-Ag(I) CP can run into the 2% agarose gel, although still near the wells, opposite to the 4% PAGE gel where majority of CoA-Ag(I) CP is adjacent to the gel wells. In comparison with the DNA molecular weight marker, both two gels confirm that the molecular weight of our prepared CoA-Ag(I) CP is much more than that of 2000 bp DNA.

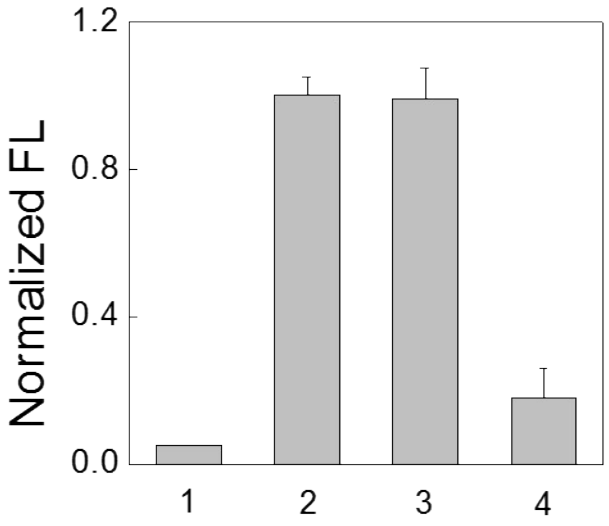

Figure S5 Fluorescence intensity at 530 nm of different SGII-stained samples. (1) SGII alone, (2) CoA-Ag(I) CP before centrifugation, (3) the supernatant of CoA-Ag(I) CP after centrifugation, and (4) the supernatant of the mixture of CoA-Ag(I) CP and GO after centrifugation. [CoA] = [Ag(I)] = 100 μM.

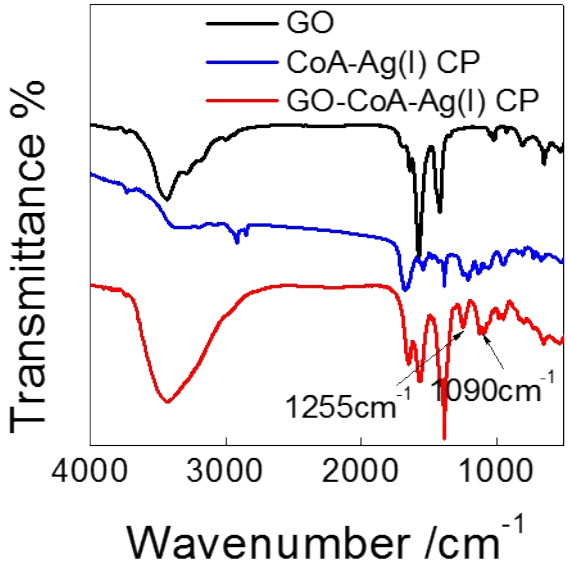

Figure S6 FT-IR spectra of GO, CoA-Ag(I) CP, and the precipitate of CoA-Ag(I) CP and GO after centrifugation. [CoA] = [Ag(I)] = 100 μM.

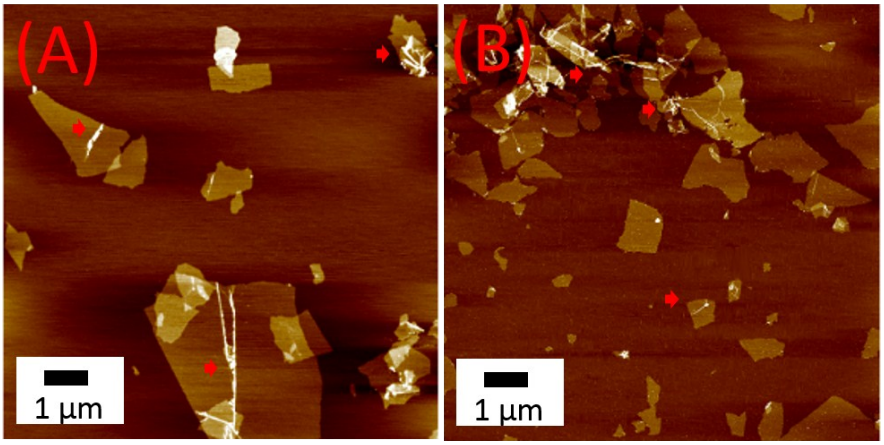

Figure S7 Atomic force microscopy (AFM) images (A and B) with enlarged scale of GO and 1 mM CoA-Ag(I) CP. The red arrows indicate the positions of CoA-Ag(I) CP.

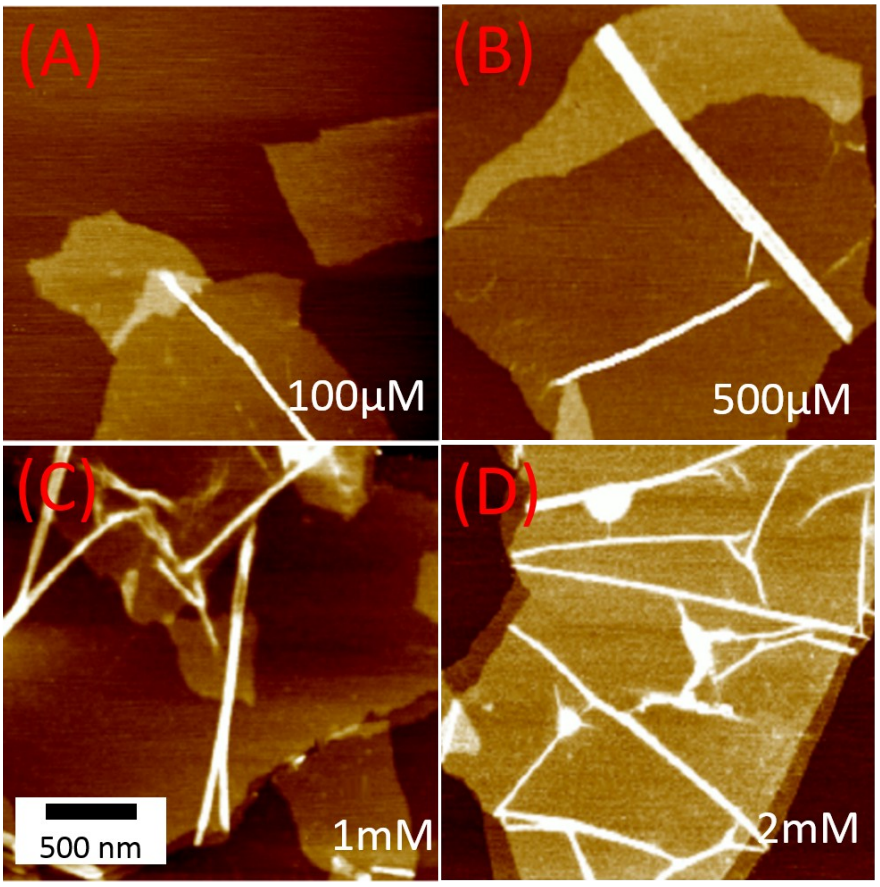

Figure S8 Atomic force microscopy (AFM) images of (A) GO and 100 μM CoA-Ag(I) CP, (B) GO and 500 μM CoA-Ag(I) CP, (C) GO and 1 mM CoA-Ag(I) CP, and (D) GO and 2 mM CoA-Ag(I) CP for demonstrating affinity interaction of CoA-Ag(I) CP and GO.

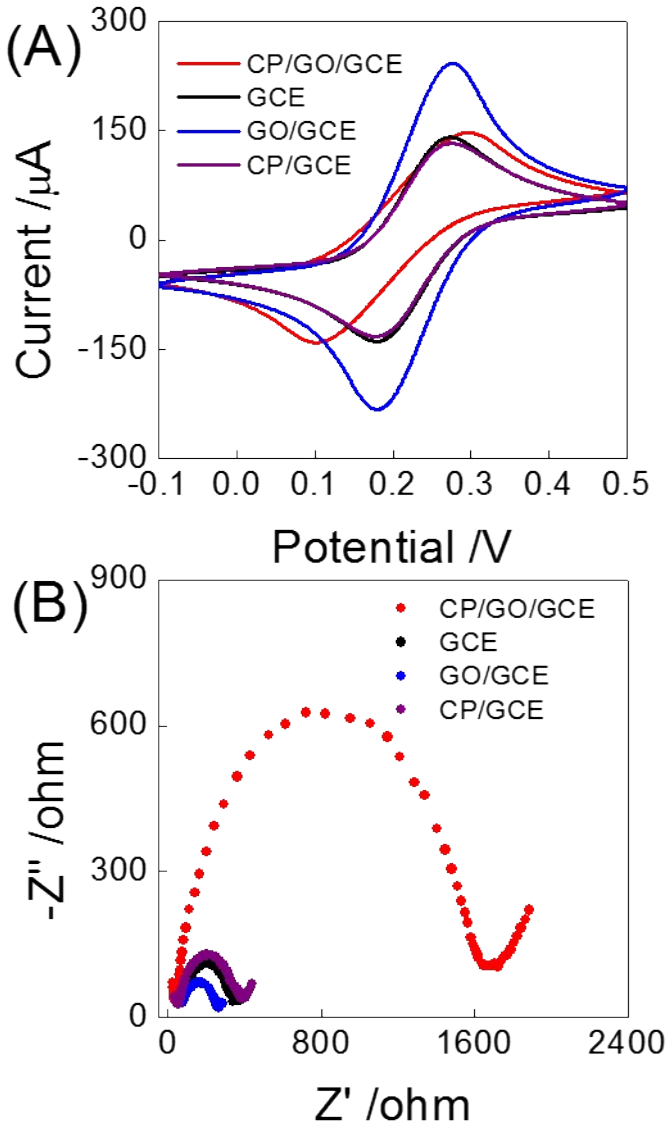

Figure S9 (A) Cyclic voltammograms of the different modified electrodes in 10 mM $[Fe(CN)_6]^{3-/4-}$ containing 0.1 M KCl with a scan rate of 50 mV·s^{-1} and (B) Electrochemical impedance spectra of the different modified electrodes with the frequency range from 10^5 to 10^{-2} Hz at amplitude of 5 mV in 10 mM $[Fe(CN)_6]^{3-/4-}$ containing 0.1 M KCl. GCE: bare GCE (black); GO/GCE: GO-electrodeposited GCE (blue); CP/GCE: CoA-Ag(I) CP-adsorbed GCE (purple); CP/GO/GCE: CoA-Ag(I) CP-adsorbed GO/GCE (red). [CoA] = [Ag(I)] = 100 μM.

We verified the adsorption of CoA-Ag(I) CP on GO by electrochemical measurements. As

illustrated in Figure S9A, compared with bare GCE (black), the cyclic voltammetry (CV) signal of $[Fe(CN)_6]^{3-/4-}$ dramatically increases with electrodeposition of GO (blue), indicating effectively accelerating electron transfer by GO modification. The CV signal sharply decreases in response to the adsorption of CoA-Ag(I) CP efficiently on the surface of GO-modified electrode (red) because of the electrostatic repulsion between anionic $[Fe(CN)_6]^{3-/4-}$ and negatively charged CP (deriving from phosphate group of CoA). However, if the CP is directly modified on the bare GCE surface (purple), the CV signal has almost unchanged, suggesting the essential role of GO on adsorption of CoA-Ag(I) CP. Electrochemical impedance spectroscopy (EIS) was employed to further monitor the modified electrodes mentioned above by electron transfer resistance (R_{et}) (Figure S9B). The bare GCE (black) shows a small semicircle and R_{et} is about 300 Ω, and the succedent GO/GCE (blue) exhibits a lower semicircle due to conductivity of GO. After CoA-Ag(I) CP is coated onto GO/GCE, a sharp increase of R_{et} is observed (red), while the diameter of semicircular part for CP/GCE (purple) is much smaller than that of CP/GO/GCE and roughly equal to that of bare GCE. These results correspond with that of aforementioned CV experiment, further indicative of the adsorption of CoA-Ag(I) CP on GO.

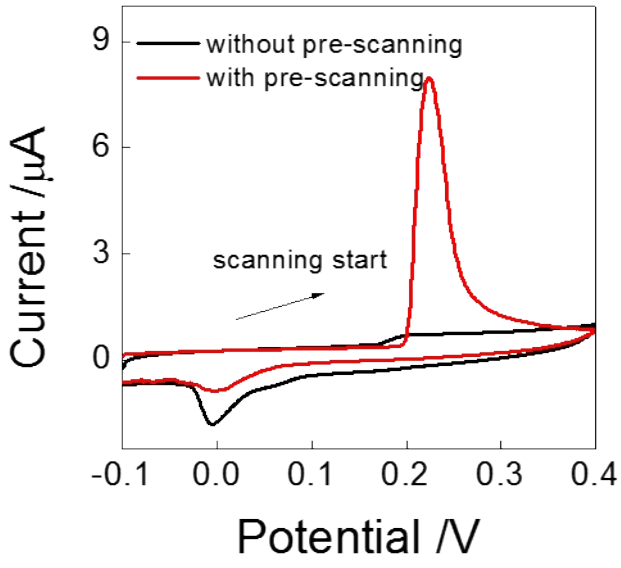

Figure S10 Cyclic voltammograms scanning from -0.1 V to +0.4 V at the CP/GO/GCE without (black) and with (red) pre-scanning for 10 cycles from -1.2 V to 0 V in N_2-saturated 100 mM PBS (pH 7.0) in the absence of H_2O_2. [CoA] = [Ag(I)] = 100 μM. (The arrow indicates the start direction of the scanning)

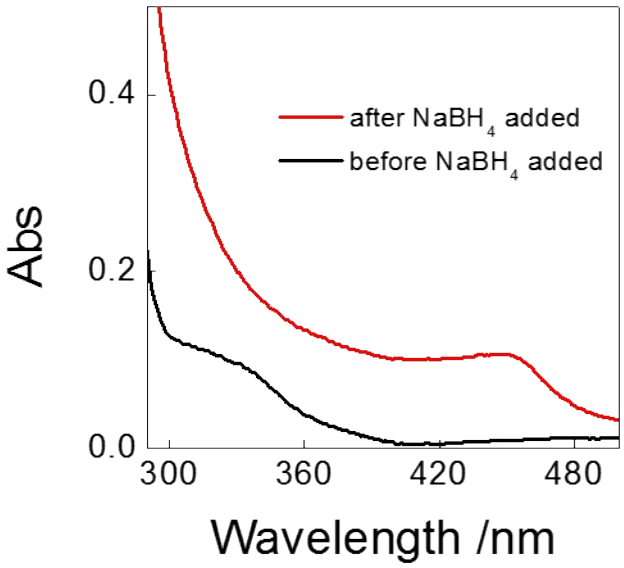

Figure S11 UV-vis absorption spectra of CoA-Ag(I) CP before (black) and after $NaBH_4$ reduction (red). [CoA] = [Ag(I)] = 100 μM.

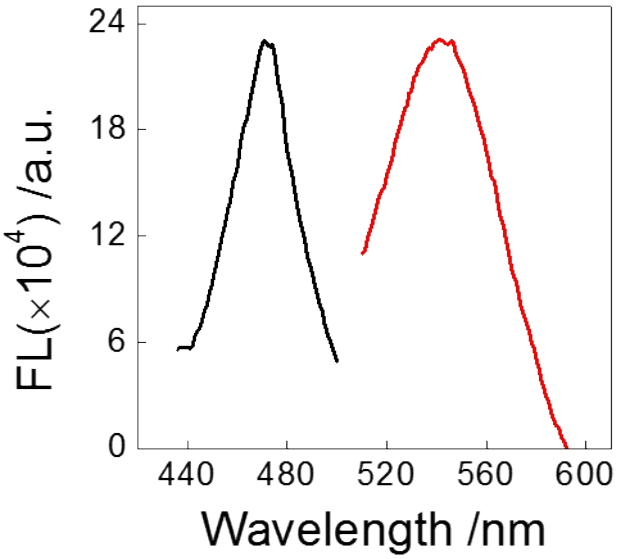

Figure S12 Fluorescence excitation (black) and emission (red) spectra of CoA capped-AgNCs prepared by reduction of CoA-Ag(I) CP by $NaBH_4$. [CoA] = [Ag(I)] = 100 μM.

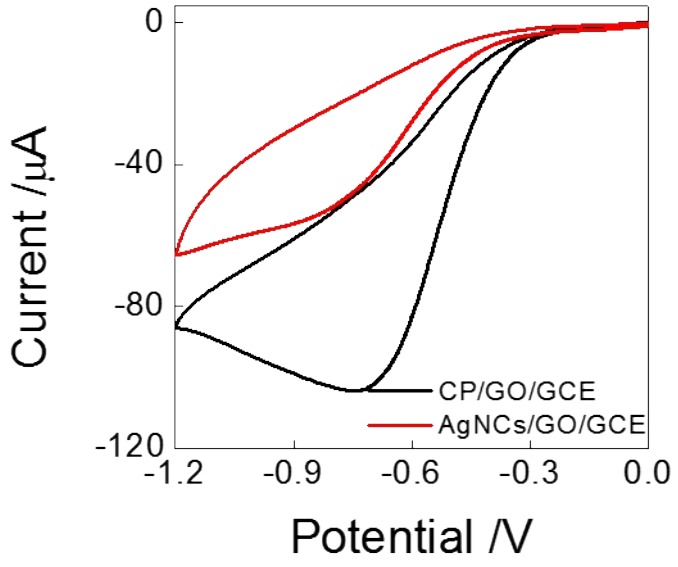

Figure S13 Cyclic voltammograms scanning from -1.2 V to 0 V at CP/GO/GCE (CoA-Ag(I)-adsorbed GO/GCE, black) and AgNCs/GO/GCE (CoA-capped AgNCs-adsorbed GO/GCE, CoA-capped AgNCs were prepared by the reduction of CoA-Ag(I) CP by $NaBH_4$, red) in N_2-saturated 100 mM PBS (pH 7.0) in the presence of 5 mM H_2O_2. [CoA] = [Ag(I)] = 100 μM.

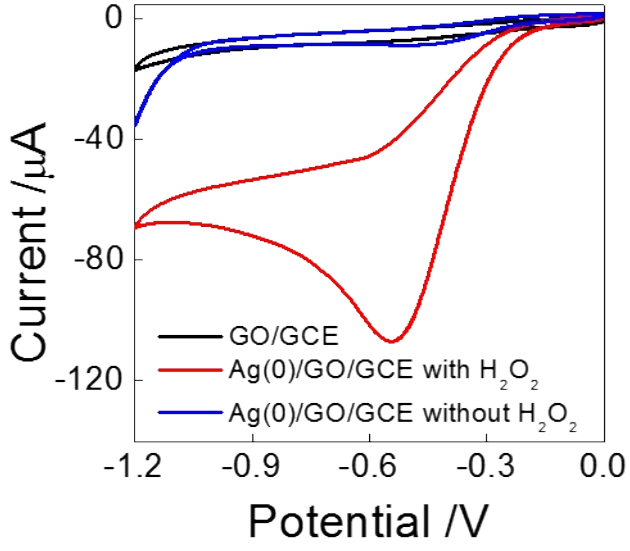

Figure S14 Cyclic voltammograms of GO-electrodeposited GCE (GO/GCE, black), Ag(0)-electrodeposited GO/GCE (Ag(0)/GO/GCE) in N_2-saturated 100 mM PBS (pH 7.0) with 5 mM H_2O_2 (red) or without 5 mM H_2O_2 (blue).

In order to further convince the Ag(0) mechanism, the electrocatalysis of Ag(0)/GO/GCE toward H_2O_2 was further investigated and the results are shown in Figure S14. We cannot observe any redox peaks at GO/GCE (black), and the reduction current of H_2O_2 at Ag(0)/GO/GCE greatly increased compared with GO/GCE and the reduction peak potential of H_2O_2 shifted positively to -0.55 V (red). Moreover, Ag(0)/GO/GCE shows negligible signal in the absence of H_2O_2. This result proved that Ag(0)/GO/GCE was also capable of electrocatalysis of H_2O_2 reduction, further supporting that the unique electrocatalytic activity of CoA-Ag(I) CP to H_2O_2 reduction is due to the Ag(0) mechanism. The reduction peak potential of H_2O_2 on Ag(0)/GO/GCE (-0.55 V) is more positive than that on CP/GO/GCE (-

0.7 V), implying the higher electrocatalytic activity of electrodeposited Ag(0) than that of adsorbed CoA-Ag(I) CP, which can be ascribed to more Ag(0) loaded on the electrode surface by the electrodeposited Ag(0) process. These results support the electrocatalytic mechanism of CoA-Ag(I) CP referred in our work and suggest that CoA-Ag(I) CP-induced electrocatalytic reduction might result from the resulting CoA-Ag(0) CP or tiny AgNCs in the electrochemical scanning process.

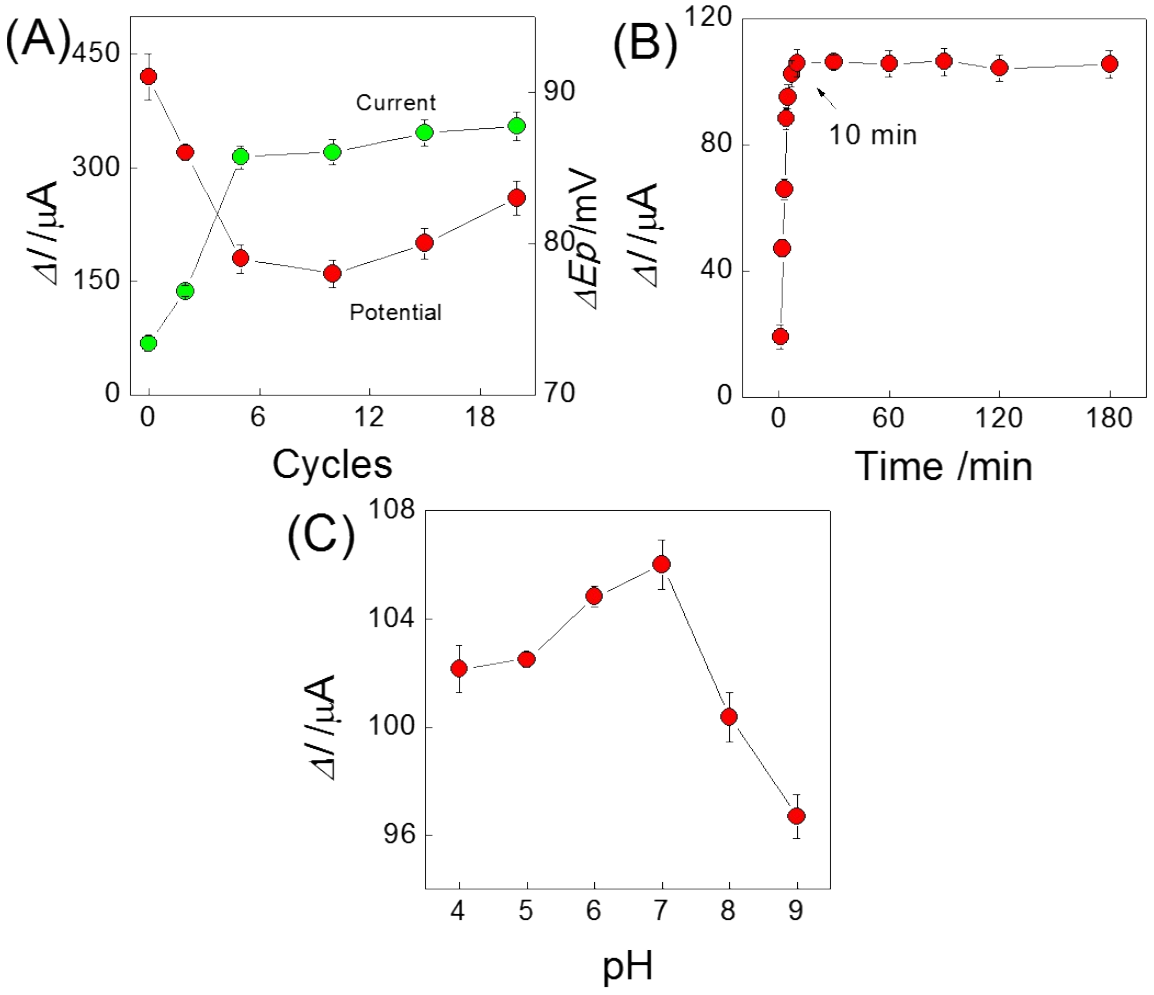

Figure S15 (A) Influence of electrodeposition cycles of GO on GCE on the current response and the anodic-to-cathodic peak separation (*ΔEp*) of the resulting GO/GCE in 10 mM $[Fe(CN)_6]^{3-/4-}$ containing 0.1 M KCl aqueous solution; (B) Influence of different absorption time (1, 2, 3, 4, 5, 7, 10, 30, 60, 90, 120, and 180 min) and (C) Effect of pH of CoA-Ag(I) CP at GO/GCE on the electrocatalytic reduction peak current of 5 mM H_2O_2 at the resulting CP/GO/GCE in N_2-saturated 100 mM PBS (pH 7.0), [CoA] = [Ag(I)] = 100 μM.

Based on the unique electrocatalytic activity of CoA-Ag(I) CP, a novel electrochemical sensor has been developed for quantitative detection of CoA. Several experimental

parameters, including electrodeposition cycles of GO on glass carbon electrode (GO/GCE), adsorption time of CoA-Ag(I) CP on GO/GCE, and pH of supporting electrolyte have been optimized for improving the performance of the electrochemical sensor. The GO/GCEs after electrodeposition were monitored by CVs with $[Fe(CN)_6]^{3-/4-}$ probe, and the results (Figure S15A) indicate that the optimal electrodeposition cycle is 10 which offers high current response with the smallest anodic-to-cathodic peak separation (*ΔEp*). Figure S15B exhibits that the response current of CV upon H_2O_2 reduction increases with the increasing adsorption time of CoA-Ag(I) CP on GO/GC and then approaches a constant value at 10 min. Thus, 10 min of adsorption time was selected in the following experiments. A further study was performed to investigate the influence of pH (Figure S15C) and the maximal reduction peak current of H_2O_2 was obtained at pH 7.0. Accordingly, a buffer solution (pH 7.0) was selected as the supporting electrolyte in the experiments.

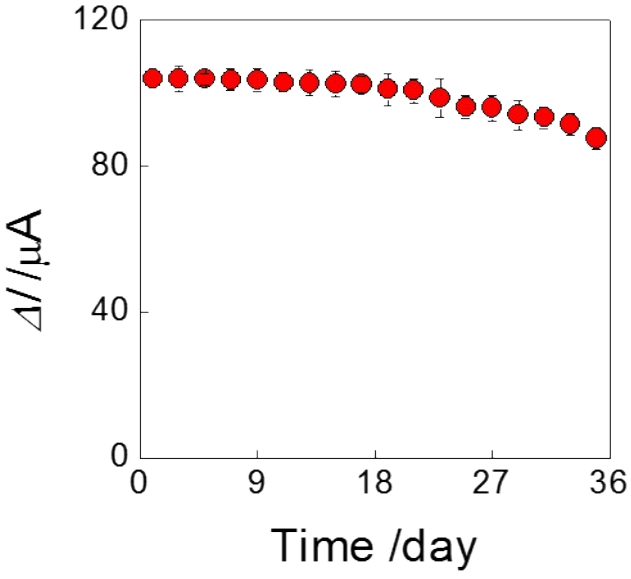

Figure S16 The stability of the proposed electrochemical sensor examined every two days in 35 days. [CoA] = [Ag(I)] = 100 μM.

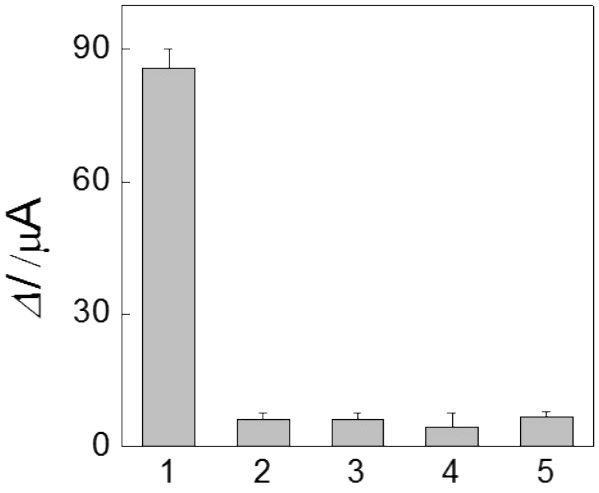

Figure S17 Electrochemical detection of p300 activity by the CoA-Ag(I) CP-based assay. The electrochemical response of the proposed assay to the full reaction mixture of Ac-CoA, the substrate peptide (P), Ag(I), and p300 (1), the same mixture as (1) without p300 (2), without Ag(I) (3), without Ac-CoA (4), or without the substrate peptide (5). [p300] = 10 nM, [Ac-CoA] = 500 μM, [peptide] = 200 μM, and [Ag(I)] = 500 μM.

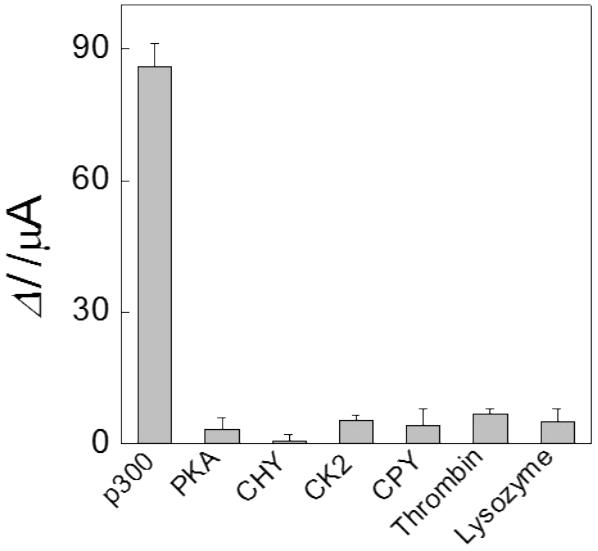

Figure S18 Selectivity of the electrochemical HAT sensor. The concentration of all analysts is 10 nM.

Table S1 Measurement of CoA spiked in 10% blood serum (v/v) by the proposed electrochemical approach.

Sample number	CoA (μM) added	Found (μM)[a]	Recovery (%)[a]	RSD(%)[a]
1	0	0	-	-
2	10	9.70	97.0	5.3
3	20	21.52	107.6	3.1
4	40	43.40	108.5	2.7
5	60	58.02	96.7	2.8
6	100	103.01	103.0	4.5

[a] the average value of three parallel determinations.

Table S2 Comparison of CoA-Ag(I) CP based HAT assay with other previously-reported HAT assays.

Detection method	HAT	Antibody-free	Label-free	Detection limit	Detection range
FRET detection based on quantum-dots[4]	p300	No	No	0.5 nM[c]	0.5-100 nM
Colorimetric assay based on enzymatic immune-assembly Au nanoparticles[5]	PCAF[a]	No	Yes	0.5 nM	2-200 nM[b]
Dual-mode FRET assay for screening HAT modulators[6]	p300	Yes	No	0.1 μM[c]	0.1-2.58 μM
Our previous fluorescence assay based on magnetic graphitic nanocapsules[7]	p300	Yes	No	0.1 nM	0.5-100 nM[b]
This proposed electrochemical HAT assay	p300	Yes	Yes	0.067 nM	0.1-100 nM[b]

[a] Histone acetyltransferase PCAF

[b] The linear range

[c] LDC: The lowest detectable concentration

Reference

1. S. William, J. R. Hummers and E. O. Richard, *J. Am. Chem. Soc.,* 1958, **80**, 1339-1339.
2. C. I. Richards, S. Choi, J. C. Hsiang, Y. Antoku, T. Vosch, A. Bongiorno, Y. L. Tzeng and R. M. Dickson, *J. Am. Chem. Soc.,* 2008, **130**, 5038-5039.
3. Y. L. Xia, W. H. Li, M. Wang, Z. Nie, C. Y. Deng and S. Z. Yao, *Talanta,* 2013, **107**, 55-60.
4. J. E. Ghadiali, S. B. Lowe and M. M. Stevens, *Angew. Chem. Int. Ed.,* 2011, **50**, 3417-3420.
5. Z. Zhen, L. Tang, H. Long and J. H. Jiang, *Anal. Chem.,* 2012, **84**, 3614-3620.
6. N. Xie, E. N. Elangwe, S. Asher and Y. J. G. Zheng, *Bioconjugate Chem.,* 2009, **20**, 360-366.
7. Y. T. Han, P. Li, Y. T. Xu, H. Li, Z. L. Song, Z. Nie, Z. Chen and S. Z. Yao, *Small,* 2015, **11**, 877-885.